Available online at www.sciencedirect.com
ScienceDirect
Journal of Nuclear Materials 363–365 (2007) 1000–1005
journal of nuclear materials
www.elsevier.com/locate/jnucmat

Structure of MARFEs and ELMs in NSTX

R.J. Maqueda [a,*], R. Maingi [b], K. Tritz [c], K.C. Lee [d], C.E. Bush [b], E.D. Fredrickson [e], J.E. Menard [e], A.L. Roquemore [e], S.A. Sabbagh [f], S.J. Zweben [e]

[a] *Nova Photonics Inc., Princeton, NJ 08540, USA*
[b] *Oak Ridge National Laboratory, Oak Ridge, TN 37831, USA*
[c] *Johns Hopkins University, Baltimore, MD 20723, USA*
[d] *University of California at Davis, Davis, CA 95616, USA*
[e] *Princeton Plasma Physics Laboratory, Princeton, NJ 08543, USA*
[f] *Columbia University, New York, NY 10027, USA*

Abstract

The fast-evolving structure of MARFEs and ELMs is observed in the National Spherical Torus Experiment (NSTX) using a fast-framing camera. It is shown that Type V ELMs, the small ELM regime in NSTX, is characterized by a poloidally propagating ionization front close to the separatrix position. The ELMs also interact with the main chamber MARFE observed in NSTX coupling its movement and partial burn-through with that of the ELM cycle. During this cycle a toroidally localized MARFE precursor is seen propagating upward along field lines at speed of the order of 15 km/s. This interaction between ELM activity and MARFEs may be responsible for slow heat pulse propagation speeds seen in the divertor region.

PACS: 52.40.Hf; 52.55.Fa; 52.70.Kz

Keywords: ELM; MARFE; NSTX; Visible imaging

1. Introduction

Edge localized modes (ELMs) have been seen in nearly all tokamaks and spherical tori since the high confinement mode of operation (H-mode) was first accessed in the early 1980s [1]. The structure of these edge modes, subject of recent studies in both MAST [2] and ASDEX Upgrade [3], is of importance for mainly two reasons. First, their localization may have an effect on the power deposition on plasma facing components ultimately affecting the performance of future large experimental devices. Second, the structure is indicative of the instability and/or processes that are involved in the ELM phenomena. In this paper we present results regarding the structure of ELMs seen in the National Spherical Torus

* Corresponding author. Present address: Nova Photonics Inc., 30 Timber Ridge, Los Alamos, NM 87544, USA. Fax: +1 609 243 2874.
E-mail address: rmaqueda@pppl.gov (R.J. Maqueda).

0022-3115/$ - see front matter © 2007 Elsevier B.V. All rights reserved.
doi:10.1016/j.jnucmat.2007.01.166

Experiment (NSTX) [4] that extend those already presented in Ref. [5].

The NSTX experiment is a low aspect ratio spherical torus with a major radius $R = 0.86$ m, a minor radius $a = 0.67$ m, elongation $\kappa \sim 2.2$, plasma currents of up to 1.5 MA, toroidal fields on axis of up to 0.6 T and neutral beam auxiliary heating of up to 7.6 MW. Plasma discharges in NSTX typically extend for 0.6–0.8 s. Of particular interest in NSTX are small ELMs, termed Type V, that result in a high performance regime with low volt-s consumption and, consequently, extended pulse lengths [6]. After an initial growth phase of the instability these small ELMs evolve into a long (0.5–1.0 ms) 'stable' phase during which characteristic edge filaments are seen. The existence space for Type V ELMs in NSTX, as well as comparison to other ELM regimes, was published in Ref. [7].

High frame rate imaging of the visible emission from the edge of magnetically confined plasmas has proved to be a very useful tool to study a number of phenomena, including ELMs [7,8]. This paper presents results from the use of a commercial digital camera that gives better-than 100 μs resolution while having a moderate-to-good pixel resolution while, at the same time, providing for over a second of recording time. The experimental setup of such a fast-framing camera in NSTX is briefly presented in Section 2. Some aspects of these small ELMs and the long-lived filaments present during them are discussed in Section 3 of this paper.

The periodic ELM activity cycle affects the divertor MARFE (multifaceted asymmetric radiation from the edge) [9], usually present inside the inner leg of the divertor, as has been previously documented in Refs. [8,10]. Interaction between ELMs and MARFEs is also seen regarding a main chamber MARFEs in which the position and structure of the MARFE responds to the ELM crash. This new phenomena is presented in Section 4. The paper concludes in Section 5 with a brief discussion.

2. Experimental setup

A Phantom 7.1 fast-framing digital camera is used in NSTX for edge physics studies. This camera can be operated at 68 000 frames/s when using 128×128 pixels or 120 000 frames/s with 64×64 pixels. Each pixel is digitized with 12 bit resolution. The exposure time can be controlled independently from the framing rate with a minimum of 2 μs and a maximum just under the inter-frame time (1/frame rate).

Digitized images are temporarily stored in on-board memory and subsequently transferred to the control computer through an Ethernet connection. With capacity to store ~87 000 128×128 pixel frames or ~350 000 64×64 pixel frames in the camera memory, full discharge coverage is possible. The fast Ethernet connection also allows for the full memory (2 GB) to be downloaded within the 10 min shot cycle between plasma discharges.

The Phantom 7.1 camera has been used in NSTX with different views of the plasma. Results from three of them are shown in this paper: a wide-angle, fish-eye elevation view of the whole plasma, a tangential view of the lower divertor region and a tangential, zoomed-in view of a ~25 cm portion of the edge just above the outer midplane of the plasma. Narrowband interference filters were used to select particular impurity or deuterium line emission wavelengths.

3. Edge localized modes

Small ELMs with energy loss per event below that measurable have been observed in different experiments. In NSTX a regime with small ELMs, termed 'Type V', has been identified [5,6]. A train of three Type V ELM events is shown in Fig. 1(a) and the evolution of the heat pulse associated with Type V ELMs as observed in the divertor region by the Phantom 7 camera shown in Fig. 1(b). Both strike point rings, inner and outer, can be seen as well as the inner leg of the divertor region. While frame #1 corresponds to the unperturbed emission, i.e., before the Type V ELM, frame #2 shows the first sign of the cycle as a secondary, or broader, outer strike point is seen (green arrow) which corresponds to the heat pulse reaching the outer target plate of the divertor. About 200 μs later a poloidally localized perturbation, associated with the ELM, enters the field of view close to its top left corner (green arrow on frame #3) and continues propagating towards the X-point (frames #4 and #5). Frame #6 shows the recovered unperturbed emission, similar to frame #1.

Fig. 2 shows the propagation of the heat pulse along the inner leg of the divertor, yielding a speed of ~1.7 km/s along the plane of the image (R, Z), and showing some (apparent) slowing down as the heat pulse approaches the X-point. Furthermore, one can infer also the propagation speed for the heat pulse if it were to be moving along a magnetic field line. Along the inner leg of the divertor the

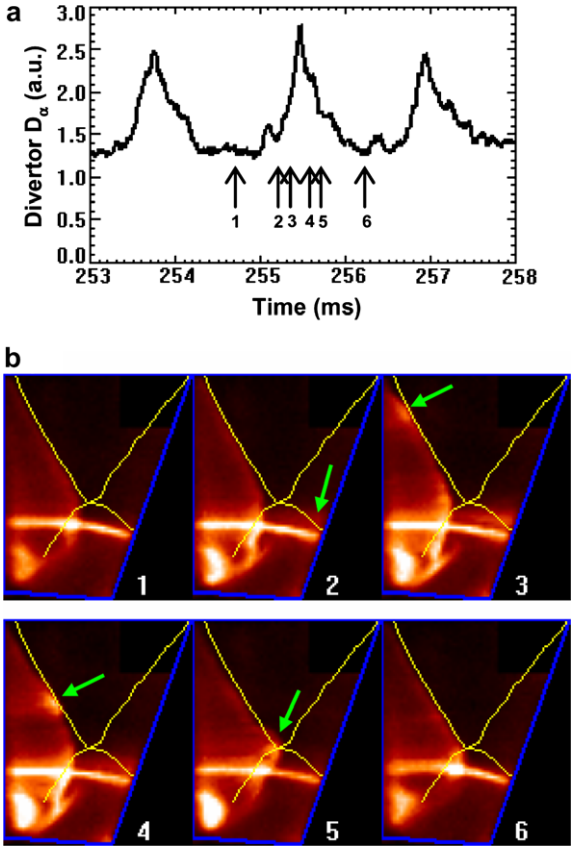

Fig. 1. Type V ELM evolution in the lower divertor region: (a) train of three ELM events as seen in the D_α emission from the lower divertor; (b) sequence of six images in CII light (6578 Å) obtained at the times indicated in part (a). The separatrix is indicated with a yellow line. The field of view for these images covers ~50 cm vertically and ~30 cm radially. (Discharge #117407, 100 000 frames/s and 5-μs long exposures.)

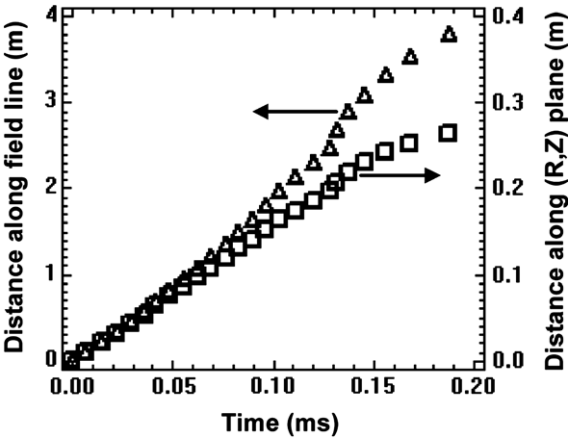

Fig. 2. Heat pulse propagation along the inner leg of the divertor during Type V ELMs. The time at which the pulse enters the field of view of the camera is assigned a value of 0 ms. The movement measured on the plane of the image is shown with squares and that corresponding to movement along the magnetic field line is shown with triangles. (Discharge #117407, 239–259 ms).

toroidal field is approximately 10 times stronger than the corresponding poloidal field resulting then in propagation at ~20 km/s along field lines. The *X*-point magnetic topology, where the poloidal field is zero, is also able to explain the slowing down observed in the *R*, *Z* plane (squares in Fig. 2).

Finally, a propagation speed of ~20 km/s along field lines would imply a temperature T_e ~4 eV, assuming this propagation occurs at the ion acoustic speed. This is the typical temperature at the foot of the H-mode pedestal and, hence, it is concluded that there is some deceleration (i.e., loss of energy) as the energy pulse propagates along the SOL from its birth location. The characteristic pedestal temperatures are ~200 eV. We should point out as a result of this measurement that the delay between the signature on the outer strike point and that on the inner leg of the divertor *cannot* be indicative of the birth location of the heat pulse as assumed in Ref. [6].

Further evidence of the poloidal localization of the Type V ELM events is shown in Fig. 3. The images in this figure show a 23×23 cm region of the poloidal plane just above the outer midplane. The Type V ELM filament is seen in this image sequence moving upwards and becoming 'aligned' to the line of sight only in frames #9–11. The structure of the filament can then be obtained from these frames: a ionization front 'ribbon' connected to the main D_α emission layer originating in gas recycling. As this ribbon moves poloidally upward (and at the same time moves toroidally in the counter-Ip direction [5]) the emission layer is displaced outwards by ~4 cm, the radial width of the ribbon. The poloidal extent of this ribbon, inferred from interferometer signals is ~13 cm of which only the front, ionizing edge is seen in D_α emission. It is also known (Ref. [5]) that the ribbon carries ~400 A of current. Given the size typical dimensions of the ribbon this current corresponds to a current density of ~80 kA/m^2, comparable to typical current densities within the edge pedestal in spherical tori. This then suggests the possibility that the Type V ELM ribbon is actually momentarily shifting the magnetic flux surface outwards re-structuring the edge pedestal, together with the D_α emission layer. This is similar to the ELM evolution presented by Kirk et al. [2] with the main differences that in NSTX rotation of the

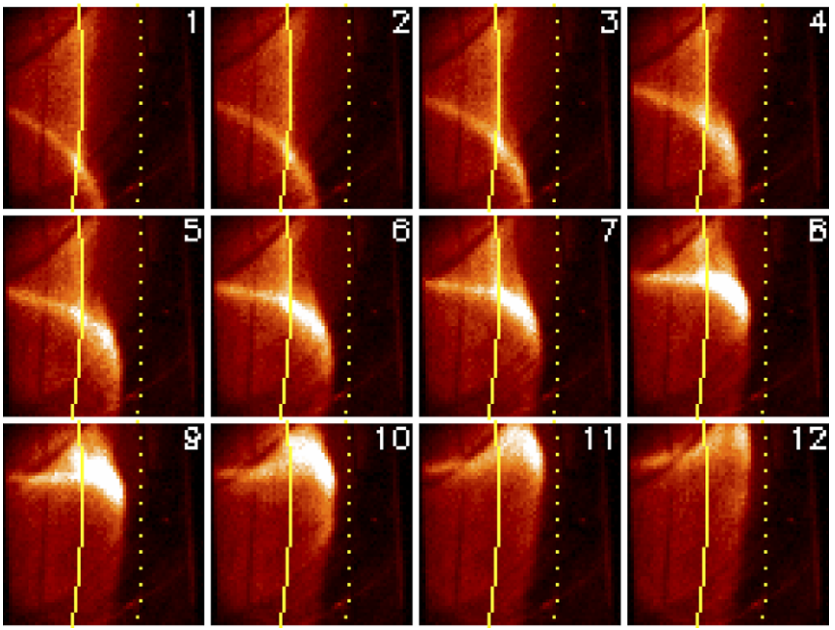

Fig. 3. Type V ELM filament imaged on the edge of NSTX. The image sequence corresponds to D_α recycling light (3 μs exposures and 120 000 frames/s) obtained on a 23 cm × 23 cm region of the poloidal plane. The separatrix position is indicated with a solid yellow line and the antenna limiter shadow is indicated with a dotted yellow line. The filament moves poloidally from the bottom left corner (frame #1 at 668.343 ms) to the top of the image (frame #12 at 668.434 ms). (Discharge #119318.)

filament is opposite to the edge plasma rotation [6] and the radial velocity is bounded to <0.2 km/s.

4. Main chamber MARFE

MARFE phenomena are routinely seen in NSTX. An example corresponding to the high-density late-phase of an H-mode discharge, is shown in Fig. 4. In this case the camera was used in the wide-angle, fish-eye view with a D_α-line bandpass filter. In Fig. 4(a) a sequence of images are shown leading to the formation of a toroidally symmetric ring (Fig. 4(b)). Only the region surrounding the center column of NSTX is shown in this sequence, with the silhouette of the 37 cm diameter center column indicated in each frame by the vertical dotted lines. These lines also correspond to 2 m in the vertical direction. A highly-radiating, poloidally and toroidally localized plasmoid is seen rotating around the center column (hidden behind this column in frame #5) and approximately following the magnetic field pitch.

The origin of the cold plasmoid seen rotating in Fig. 4(a) is similar to a MARFE: impurity emission only balanced by thermal conduction. Nevertheless, as it will be discussed further down in this section, there is an imbalance in the parallel energy flows on the upstream (larger) and downstream (smaller) sides of this plasmoid. This imbalance then causes the decay of the cold and dense plasma at the upstream edge while the downstream edge grows. Such dynamic, apparent (wave-like) motion [11] is possible with this plasmoid near the thermal stability condition. The corkscrew, upward movement eventually stagnates, hence departing from the magnetic field pitch and, in this case, forming a commonly observed toroidally symmetric MARFE ring. Since the equilibrium position of this ring, with the ion ∇B-drift direction downward, is close to the lower X-point [12] the MARFE migrates downward as shown in Fig. 4(b). It should be pointed out that, although a MARFE with a short poloidal extension is seen in this example (5–10 cm), rings with longer poloidal dimensions (up to ~40 cm) have also been observed.

The toroidal localization of the MARFE precursor as shown in Fig. 4(a) has not been previously observed. This localization and rotation is shown again in Fig. 5(a). In this case a ~56-cm wide region (18 pixels) around the center column is shown as a function of time, similar to a 'wide-slit streak' exposure. The localization and rotation of the MARFE precursor appears then on this 'film strip' as a tilted corkscrew structure, for example at around 662 ms.

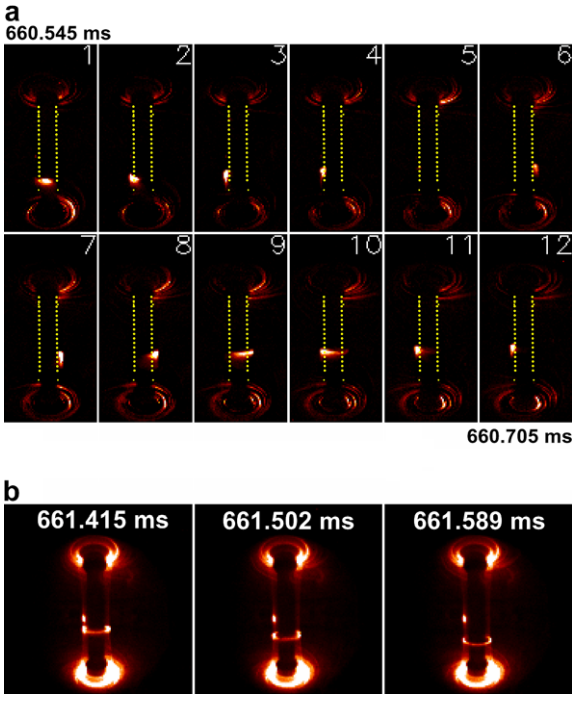

Fig. 4. MARFE evolution in high-density NSTX discharge (#117125): (a) Images of center stack and divertor regions showing toroidally localized MARFE precursor moving upward, rotating around center column and (b) fish-eye view of NSTX with conventional toroidally symmetric MARFE ring moving downward. For contrast enhancement in part (a) an 'average frame' has been subtracted from each frame. The images shown cover the 660.545 ms (top left) to 660.705 ms (bottom right) period with 9 μs exposures at 68 000 frames/s.

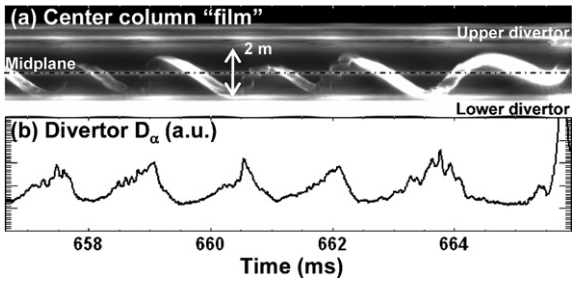

Fig. 5. Interaction between ELMs and MARFEs in the same discharge as Fig. 4 (#117125): (a) 'streak'-like image obtained with a ~56-cm wide 'slit' around the center column and (b) the lower divertor D_α light monitor. The MARFE moves up and down in response to the ELM activity.

The up/down movement of the MARFE and its precursor is also clearly seen in Fig. 5(a).

Fig. 5 also shows the interaction between the MARFE and ELMs. In Fig. 5(b) the D_α recycling light monitor from the lower divertor region is shown with the same time base as the film strips of the inner column of NSTX (Fig. 5(a)). The periodic increases in D_α light seen in Fig. 5(b) are generally associated with ELMs (see Section 3), in this case small events with some characteristics of Type III. It is then seen in this figure that, as the divertor recycling light increases due to the heat pulse on open field lines associated with the ELM event (Section 3), the MARFE precursor initiates its upward movement only after a short delay. It is then conjectured that a portion of the ELM heat pulse, still within the closed field line region, is responsible for the heat imbalance causing this movement. Depending on the amount of energy released during the ELM event the movement stagnates at a different vertical position. Despite the different vertical position of this stagnation, the downward movement occurs at a constant (and uniform between cycles) speed, governed by the ion ∇B-drift. Finally, we point out that the last ELM of the cycle shown is a bigger event (a Type I ELM) which at first causes the MARFE to slow down and reverse its downward movement (~665.5 ms) and later on burns through the highly emitting lithium-like states within the MARFE plasmoid and, hence, dissipating the MARFE.

5. Discussion

An interpretation has emerged from the material in Ref. [5] and that presented here that the Type V ELMs in NSTX are characterized by ribbon like filaments moving poloidally and toroidally. These filaments evolve during a long 'quasi-stable' phase that can reach 1 ms in duration and during which the filament, with electron temperature and density comparable to those inside the edge pedestal, is still connected to the main core plasma. In fact, during this long stable phase (much longer than parallel transport times to the divertor target plates for the 100–200 eV plasma contained within the filament), the filament is in itself a re-structuring of the pedestal, including a local momentary shift outward of the magnetic surfaces on a time scale of ~100 μs producing the appearance of a moving 'lip' (frames #7–11 of Fig. 3). We point out that the filament lifetime is much longer than that of the Type I ELM filament observed in MAST which has a <0.1 ms long 'attached' phase [2]. Is not yet known in NSTX at what point in time or by which mechanism the filament 'breaks-off' its connection to the pedestal. It is possible, nonetheless, that the filament actually

decays in time and the small ELM crash characteristic of the Type V ELMs, with an energy loss per event of <1% of the plasma stored energy, is a result of enhanced transport during the 0.5–1 ms of the filament lifetime. This energy loss mechanism is similar to what is postulated for the initial, attached phase of the ELM crash in MAST [2], which may also involve perturbation of the E_r well as in Ref. [13]. In NSTX, support for this is given by the observation that the enhanced divertor recycling light is coincident in time with the presence of the hot, dense, current carrying filament and has no sharp increase in time through its ~1 ms long evolution [$\geqslant$200 μs risetime, Fig. 1(a)]. In contrast, for instance, MAST's divertor D_α signatures have a ~50 μs risetime [2].

Another important aspect of the ELM activity in NSTX is its interaction with main chamber MARFEs as presented in connection to Figs. 4 and 5. It is clear from these figures that the toroidally symmetric MARFE has as precursor a high density seed region that is toroidally localized and that moves up (and in some cases down) the center stack of NSTX in response to the ELM activity. This seed precursor is in itself a remnant of a preceding MARFE and product of its partial burn-through. Such an interaction between the ELM crash and the main chamber MARFE provides a mechanism to explain the slow propagation speed for the Type V ELM heat pulse observed on the inner leg of the divertor region (Fig. 2).

Acknowledgments

This work was supported by US D.O.E. Contract Nos. DE-FG02-04ER54520, DE-AC05-00OR22725 and DE-AC02-76CH03073.

References

[1] F. Wagner et al., Phys. Rev. Lett. 49 (1982) 1408.
[2] A. Kirk et al., Phys. Rev. Lett. 96 (2006) 185001.
[3] B. Kurzan et al., Phys. Rev. Lett. 95 (2005) 145001.
[4] S.M. Kaye et al., Nucl. Fusion 45 (2005) S168.
[5] R. Maingi et al., Phys. Plasmas 13 (2006) 092510.
[6] R. Maingi et al., Nucl. Fusion 45 (2005) 264.
[7] R. Maingi et al., Nucl. Fusion 44 (2005) 1066.
[8] N. Nishino et al., J. Plasma Fus. Res. 78 (2002) 1278.
[9] B. Lipschultz et al., Nucl. Fusion 24 (1984) 977.
[10] N. Nishino et al., Trans. Inst. Electr. Eng. Jpn. A (Japan) 125A (2005) 902.
[11] A.V. Chankin, Phys. Plasmas 11 (2004) 1484.
[12] N. Asakura et al., Nucl. Fusion 36 (1996) 795.
[13] M.R. Wade et al., Phys. Rev. Lett. 94 (2005) 225001.